Right ventricular area strain from 3D echocardiography: mechanistic insight of right ventricular dysfunction in pediatric pulmonary hypertension

Pei-Ni Jone, Nicolas Duchateau, Zhaoxing Pan, Dunbar Ivy, Pamela Moceri

▶ **To cite this version:**

Pei-Ni Jone, Nicolas Duchateau, Zhaoxing Pan, Dunbar Ivy, Pamela Moceri. Right ventricular area strain from 3D echocardiography: mechanistic insight of right ventricular dysfunction in pediatric pulmonary hypertension. The Journal of Heart and Lung Transplantation, 2020. hal-03088218

HAL Id: hal-03088218
https://hal.science/hal-03088218v1

Submitted on 25 Dec 2020

HAL is a multi-disciplinary open access archive for the deposit and dissemination of scientific research documents, whether they are published or not. The documents may come from teaching and research institutions in France or abroad, or from public or private research centers.

L'archive ouverte pluridisciplinaire **HAL**, est destinée au dépôt et à la diffusion de documents scientifiques de niveau recherche, publiés ou non, émanant des établissements d'enseignement et de recherche français ou étrangers, des laboratoires publics ou privés.

Preprint version accepted to appear in The *Journal of Heart and Lung Transplantation*.
Final version of this paper available at https://www.sciencedirect.com/science/article/abs/pii/S1053249820318313

Right Ventricular Area Strain from 3D Echocardiography: Mechanistic Insight of Right Ventricular Dysfunction in Pediatric Pulmonary Hypertension

Pei-Ni Jone MD[1], Nicolas Duchateau PhD[2], Zhaoxing Pan MD PhD[3], D. Dunbar Ivy MD[1], Pamela Moceri MD PhD[4]

[1]Pediatric Cardiology, Children's Hospital Colorado, University of Colorado School of Medicine, Aurora, Colorado

[2]Creatis, CNRS UMR5220, INSERM U1206, Université Lyon 1, France.

[3]Biostatistics and Informatics, Colorado School of Public Health, University of Colorado, Denver, Colorado

[4]Universite Côte d'Azur, UR2CA, Inria Epione Team, Department of Cardiology, Hôpital Pasteur, CHU de Nice, France

Corresponding Author:

Pei-Ni Jone MD

Mailing Address:

13123 East 16th Avenue, B100, Aurora, Colorado 80045

Telephone: +1-720-777-2944

Fax: +1-720-777-7290

E-mail: pei-ni.jone@childrenscolorado.org

Preprint version accepted to appear in The *Journal of Heart and Lung Transplantation*.
Final version of this paper available at https://www.sciencedirect.com/science/article/abs/pii/S1053249820318313

Background: Right ventricular (RV) function is a major contributor to the outcome of pulmonary arterial hypertension (PAH). Adult studies demonstrated that regional and global changes in RV deformation are prognostic in PAH using 3-dimensional echocardiography (3DE). However, regional and global dynamic changes in RV mechanics have not been described in pediatric PAH. We compared 3DE RV regional and global deformation between pediatric patients who had associated PAH with congenital heart disease (APAH-CHD), pediatric patients who had idiopathic PAH (IPAH), and normal controls, and evaluated the clinical outcomes.

Methods: A total of 48 controls, 47 patients with APAH-CHD, and 45 patients with IPAH were evaluated. 3DE RV sequences were analyzed and post-processed to extract global and regional deformation (circumferential, longitudinal, and area strain). Statistical analyses compared the sub-groups on the basis of global and regional deformation, and outcome analysis was performed.

Results: Patients with PAH had significantly different global and regional deformation ($p < 0.001$) compared with controls. Patients with APAH-CHD and and those with IPAH significantly differed in global circumferential strain ($p < 0.010$), area strain (inlet septum, $p = 0.041$), and circumferential strain at the inlet septum ($p < 0.019$), apex free wall ($p < 0.004$), and inlet free wall ($p < 0.004$). Circumferential strain at the inlet free wall and circumferential, longitudinal, and area strain at the apex free wall were predictors of adverse events.

Conclusion: RV regional and global strain differ between controls and pediatric patients with PAH. RV apical free-wall area strain provides insight into the mechanism of RV dysfunction in pediatric patients with PAH, with regional strains emerging as outcome predictors, suggesting that this novel measure may be considered as a future measure of RV function.

Preprint version accepted to appear in The *Journal of Heart and Lung Transplantation*.
Final version of this paper available at https://www.sciencedirect.com/science/article/abs/pii/S1053249820318313

Keywords: Three-dimensional echocardiography; right ventricular area strain; pediatric pulmonary hypertension; clinical outcomes; ventricular function; prognosis

INTRODUCTION

Right ventricular (RV) function is crucial for survival in pediatric pulmonary arterial hypertension (PAH).[1,2] RV longitudinal strain (RVLS) using 2-dimensional (2D) speckle tracking echocardiography is a quantitative way to detect abnormal ventricular function in PAH and has been used to evaluate for outcomes.[2–4] The limitation of RVLS from a single RV view is 1-dimensional in the longitudinal fashion and does not yield a true global view of the RV function. Evaluation of RV function using 2D echocardiography (2DE) is limited owing to the complex shape of the right ventricle. Recent studies have used 3 RV-focused apical views to reconstruct a global view of the right ventricle to evaluate the RV function.[5,6] However, multiple imaging planes from 2DE are needed to integrate the asymmetrical shape of the right ventricle, making the quantification of the right ventricle difficult and impractical.

The 3-dimensional (3D) echocardiography (3DE) captures the right ventricle in 1 pyramidal dataset, allowing for evaluation of the RV shape, size, and function without geometric assumptions.[7–9] The right ventricle can be divided into the septal and free-wall areas from 3DE datasets.[8] The segmentation of the RV septal and free-wall areas can be further divided into the inlet, outlet, body, and apex (Figure 1) to study the different regions of the right ventricle. Area strain combines the contribution of the longitudinal and circumferential deformations to provide the regional and global evaluation of the right ventricle from the 3DE datasets. Studies on adults have demonstrated that regional and global area changes (referred to as area strain), derived from

Preprint version accepted to appear in The *Journal of Heart and Lung Transplantation*.
Final version of this paper available at https://www.sciencedirect.com/science/article/abs/pii/S1053249820318313

3DE datasets, in RV deformation can be used for prognostic evaluation in PAH.[9,10] However, these regional and global dynamic changes in RV mechanics have not yet been described in pediatric pulmonary hypertension (PH). We have previously demonstrated that 3D RV ejection fraction (EF) and free-wall RVLS (2D cut plane from the 3D datasets) are prognostic in evaluating RV function in pediatric PAH.[2] As an extension of our previous study, an in-depth evaluation of regional and global RV area strain may help us understand the mechanism of RV failure. In this study, we (1) compared 3DE RV regional and global deformation between pediatric controls, pediatric patients who had associated PAH (APAH) with congenital heart disease (CHD), and those who had idiopathic PAH (IPAH) and (2) evaluated for associated clinical outcomes.

METHODS

Study population

The pediatric patients with PAH were prospectively recruited from July 2014 to October 2018 at Children's Hospital Colorado (Aurora, CO). Patients were included if they (1) had a diagnosis of IPAH or APAH-CHD by the PH specialist, (2) had a routine 2DE in addition to 3DE, and (3) were seen in the PH clinic. Patients were excluded if they were aged >18 years, if the echocardiographic acoustic window was poor, or if they had arrhythmias. Medical record data collected were body surface area (BSA), World Health Organization Functional Classifications (WHO FCs), sex, medications, heart rate, and routine 2DE parameters of RV systolic pressure from tricuspid regurgitation velocities and tricuspid annular plane systolic

Preprint version accepted to appear in The *Journal of Heart and Lung Transplantation*.
Final version of this paper available at https://www.sciencedirect.com/science/article/abs/pii/S1053249820318313

excursion (TAPSE). Echocardiograms at enrollment of the study were used, and patients were evaluated for outcomes.

Pediatric patients serving as controls had no cardiac defects or family history of cardiac disease. They were recruited from the outpatient clinic, referred either for a heart murmur, chest pain, or syncope with a normal heart structure. This study was approved by the institutional review board at the University of Colorado with informed consent obtained. A data transfer agreement with Université Côte d'Azur (Nice, France) was signed to coordinate RV area strain analysis.

The 3D Transthoracic Echocardiography

An apical 4-chamber single beat full volume dataset focused on the right ventricle (required volume rate of ≥16) was acquired in each patient and control using a 4Z1c matrix-array transducer (frequency bandwidth, 1.5–3.5 MHz; maximum depth, 30 cm; maximum field of view, 90° × 90°) on the Siemens SC2000 cardiac ultrasound system (Siemens Healthcare, Erlangen, Germany). 3DE RV datasets were acquired prospectively at the routine clinic visits and as part of Children's Hospital Colorado PH echocardiography protocol. 3DE RV datasets were digitally analyzed offline using the commercial software 4-dimensional RV Function 2.0 (TomTec Imaging Systems, Unterschleissheim, Germany) to estimate RV volumes and function automatically: 3D end-diastolic volume (EDV), 3D end-systolic volume (ESV), 3D stroke volume, and 3D EF.

RV Deformation Analysis

Deidentified 3D RV datasets were sent to Université Côte d'Azur for deformation analysis of the RV endocardial surface using computations similar to the ones published for adult

Preprint version accepted to appear in The *Journal of Heart and Lung Transplantation*.
Final version of this paper available at https://www.sciencedirect.com/science/article/abs/pii/S1053249820318313

patients with PAH (MATLAB and VTK/C++ custom software).[9] RV meshes provided by the commercial software were post-processed to extract wall deformation at each mesh vertex (circumferential, longitudinal, and area strain). The right ventricle was divided according to anatomic regions definition (Figure 1): RV inlet, RV outlet, body, and apex in both septum and free walls.7,8 This division was performed on a single reference mesh and propagated to the whole population using the point-to-point correspondences between all the meshes provided by the commercial software. On the basis of this, deformation values were available for each patient both at each point of the mesh (referred to as deformation patterns) and averaged over each of the 8 regions or the whole right ventricle (referred to as regional and global deformation values). This post-processing step to obtain area, circumferential, and longitudinal strain is fully automatic.

Clinical Outcomes

Clinical outcomes were analyzed in all patients with PAH with predefined adverse clinical events. An adverse clinical event was defined as (1) new initiation of intravenous prostacyclin, (2) PAH-related hospitalization with increased RV failure or hemoptysis, (3) creation of an atrial septostomy, (4) performance of a Pott's shunt, (5) performance of lung transplantation, or (6) death. These adverse clinical outcomes were composite end-points such as previous medication trials in PAH.[11] All patients were followed up until the clinical event or the end of the study period.

Statistical Analysis

Analyses were performed using SAS 9.4. Variables were checked for the distributional assumption of normality using normal plots, in addition to Kolmogorov–Smirnov and Shapiro–Wilk tests. For a few strain outcome measures in 1 or 2 groups, the normality assumptions were

Preprint version accepted to appear in The *Journal of Heart and Lung Transplantation*.
Final version of this paper available at https://www.sciencedirect.com/science/article/abs/pii/S1053249820318313

violated by these tests. However, the residual analysis indicated that normality assumptions for the analysis of variance (ANOVA)/analysis of covariance models are appropriate. For ease of clinical interpretation, parametric results are reported in the main text, and non-parametric results as a sensitivity analysis are reported in Supplementary Tables (available online at www.jhltonline.org). All continuous variables are reported as mean with corresponding SDs (or SEs for adjusted analysis).

Parametric analysis of covariance was used to make comparisons between controls, patients with IPAH, and patients with APAH-CHD PAH using pair-wise between-group comparison, adjusting for age, sex, and BSA. Non-parametric rank transformation ANOVA was also performed to compare the 3 groups. Kaplan–Meier survival curve was used to describe the survival behavior of time from echocardiographic study to composite outcome (see clinical outcome section for the definition of the outcome). Associations of regional and global area strain with outcomes were assessed using Cox regression model while adjusting for age and BSA of patients. The discriminating ability of Cox regression model was assessed by time-dependent integrated area under receiver operating characteristic (ROC) curve and Uno's concordance statistic (c-statistic).12 Integrated area under ROC curves is a summary statistic for the area under ROC curves of the follow-up period, and this was performed in all regional and global RV deformations. All patients were followed up to the adverse event or the end of the study (October 2018). Significance was based on an α-level of 0.05.

For visualization and understanding purposes, deformation patterns were also displayed over the average mesh for each sub-group, obtained by standard computations (Generalized Procrustes analysis). Sub-group differences were visualized in terms of median pattern over each sub-group, and statistical significance was assessed using p-value from Hotelling's T-test at each

Preprint version accepted to appear in The *Journal of Heart and Lung Transplantation*.
Final version of this paper available at https://www.sciencedirect.com/science/article/abs/pii/S1053249820318313

mesh location. Intraobserver and interobserver variabilities were performed in 30 patients (10 from each group) using Bland–Altman analysis.

RESULTS:

A total of 47 patients with APAH-CHD, 45 patients with IPAH, and 48 controls were included in this study. There were overlapping populations with PAH from our previous study.[2] There were 10 pediatric controls added from the original 38 controls from the previous study and 11 patients with IPAH added since 2016 (previous 34 patients with IPAH). The first 48 patients with APAH-CHD were included since 2014 and met the inclusion criteria so that the 3 groups had a similar sample size. One patient was excluded from patients with APAH-CHD owing to age (>18 years), thus leaving 47 patients in the APAH-CHD group.

Patients' baseline characteristics are summarized in Table 1. The etiology of the APAH-CHD group comprised 14 atrial septal defects status post repair (s/p repair), 5 ventricular septal defects s/p repair, 12 atrioventricular septal defects s/p repair, 6 patent ductus arteriosus s/p repair, 2 coarctations s/p repair, 1 transposition of the great artery s/p repair, 1 partial anomalous pulmonary venous return s/p repair, 2 total anomalous pulmonary venous return s/p repair, and 1 shone's complex s/p repair. There were more patients with WHO FC II in the IPAH group than there were in the APAH-CHD group. The 3 groups of patients were not homogeneous with respect to age, sex, and BSA (Table 1); however, these variables were adjusted in the statistical analysis. The differences in heart rates among the groups were not statistically significant. There were significant differences in TAPSE between the patients with IPAH and those with APAH (2.0 ± 0.5 vs 1.5 ± 0.5, $p < 0.001$) and between controls and patients with APAH (1.9 ± 0.4 vs 1.5 ± 0.5, $p < 0.001$); however, TAPSE was not statistically different between the patients with

Preprint version accepted to appear in The *Journal of Heart and Lung Transplantation*.
Final version of this paper available at https://www.sciencedirect.com/science/article/abs/pii/S1053249820318313

IPAH and controls (2.0 ± 0.5 vs 1.9 ± 0.4, $p < 0.488$). The RV systolic pressure estimated from tricuspid regurgitation velocity was higher in patients with IPAH than in those with APAH and in controls (71.5 ± 29.6, –38.4 ± 19.4, and 16.6 ± 3.6, respectively; $p < 0.001$). Patients with IPAH had the lowest 3D RV EF among the 3 groups (43.9 ± 7.4, 47.5 ± 5.4, 55.3 ± 4.4; $p < 0.001$). Patients with IPAH had higher pulmonary artery pressures and pulmonary vascular resistance index than patients with APAH-CHD (Table 1).

Controls and patients with PAH had significantly different RV global and regional deformation ($p < 0.001$) (Table 2, Figure 2, and see Supplementary Table S1 online [after adjusting for age, sex, and BSA]). Specifically, the global area strain was statistically different between controls and patients with PAH (mean ± SD = –29.8 ± 6.0% in controls, –24.8 ± 4.8% in those with APAH-CHD, and –22.3 ± 8.5% in those with IPAH; $p < 0.001$) (Table 2). The inlet septum area strain (–18.7 ± 7.0% vs –14.9 ± 9.7%, $p = 0.041$) and circumferential strain (–12.9 ± 4.9% vs –9.5 ± 7.5%, $p = 0.019$) were different between patients with IPAH and those with APAH. The apex free wall area strain (–24.5 ± 5.6% vs –21.4 ± 9.2%, $p = 0.037$) and circumferential strain (–13.1 ± 3.9% vs –10.3 ± 5.3%, $p = 0.004$) were also different between patients with IPAH and those with APAH. A difference was also found in the inlet free-wall circumferential strain (–15.5 ± 5.0% vs –12.3 ± 5.9%, $p = 0.004$) between the 2 groups of patients with PH (Table 2). The regional differences were confirmed by the visualization of 3D patterns in Figure 2. Global circumferential strain (–14.3 ± 3.4% vs –12.1 ± 5.0%, $p = 0.010$) were also statistically different between patients with APAH-CHD and those with IPAH (Table 2). Both parametric and non-parametric ANOVA produced consistent results among the 3 groups (see Supplementary Tables S1 and S2 online).

Preprint version accepted to appear in The *Journal of Heart and Lung Transplantation*.
Final version of this paper available at https://www.sciencedirect.com/science/article/abs/pii/S1053249820318313

Clinical Outcomes

The median follow-up was 29.4 months for all patients, 42.4 months for patients with APAH-CHD, and 21.6 months for patients with IPAH. There were 22 events (2 in patients with APAH-CHD and 20 in patients with IPAH): 9 patients with the initiation of intravenous prostacyclin, 5 patients with PAH-related hospitalization with increased RV failure or hemoptysis, 2 patients underwent atrial septostomy, 2 patients had Pott's shunt, and 4 patients died. Univariate survival analysis of regional strain, global strain, and WHO FC after adjusting for age and BSA is summarized in Table 3 for statistically significant variables and in Supplementary Table S3 (online) for all variables. The area strain of the apex free wall, the circumferential strain of the apex free wall, the longitudinal strain of the apex free wall, and the circumferential strain of the inlet free wall were predictors of adverse clinical events (Figure 3 and Table 3). Multiple Cox regression analysis demonstrated that circumferential strain at the apex free wall had a time-dependent integrated area under the curve (AUC) (iAUC) of 0.72 and Uno c-statistic of 0.72. The adjusted hazard ratio for a 1-U change in the circumferential strain at the apex free wall is 1.098 (95% CI: 1.021–1.181, p = 0.0118). Table 4 presents the Uno c-statistic summary for the 4 RV regional strain parameters. Receiver operating curves showed that the AUC for circumferential strain at the apex free wall was highest when compared with those of the other regions of the right ventricle at 24 months (Figure 4). Comparison of c-statistics between these 4 regional strain parameters showed no statistically significant differences (see Supplementary Table S4 online); however, circumferential strain at the apex free-wall iAUC was higher than that at the rest of the parameters (Table 4).

Preprint version accepted to appear in The *Journal of Heart and Lung Transplantation*.
Final version of this paper available at https://www.sciencedirect.com/science/article/abs/pii/S1053249820318313

DISCUSSION:

Our study demonstrates the regional and global RV strain differences between pediatric controls, pediatric patients with IPAH, and pediatric patients with APAH-CHD. More specifically, patients with APAH-CHD and those with IPAH mainly differed regarding the area strain (global and inlet septum) and the circumferential strain (inlet septum, inlet free wall, and apex free wall). Finally, the area strain of the apex free wall, the circumferential strain of the apex free wall, the longitudinal strain of the apex free wall, and the circumferential strain of the inlet free wall were predictors of adverse clinical events. Apex free wall is affected the most when patients have poor outcomes.

Previous studies on adults have described the value of 3D assessment of the right ventricle because the right ventricle cannot be completely evaluated in 2D.[9,10,13–15] In particular, 3D analysis incorporates the circumferential, longitudinal, and area strain to evaluate the RV systolic function and changes in RV shape.[10,14,15] Our study demonstrated results similar to the studies on adults regarding the differences of the area strain in controls compared with those in the 2 groups of patients with PAH.[9,10] Area strain provides a summary of the RV deformation, partially related to the combination of longitudinal and circumferential strain, and does not require the definition of local anatomic directions that may be prone to computational errors.

We further evaluated the differences between the regional strains of the 2 sub-groups with PAH because the etiology of pediatric patients with PH comprised mostly of patients with APAH-CHD and those with IPAH. We found that patients with IPAH and those with APAH-CHD differed in terms of circumferential strain and ventricular shape. Patients with IPAH tended to have a more dilated right ventricle than patients with APAH-CHD. This is because patients with IPAH, in general, have worse PH when than patients with APAH-CHD.[1,2] The

Preprint version accepted to appear in The *Journal of Heart and Lung Transplantation*.
Final version of this paper available at https://www.sciencedirect.com/science/article/abs/pii/S1053249820318313

circumferential fibers in the normal right ventricle are thin and located in the sub-epicardium, and it is possible that these fibers are stretched with a subsequent reduction in contractility when the right ventricle becomes more dilated in patients with IPAH.[14,16] Previous studies have demonstrated that the inflow region of the RV free wall has greater fiber shortening and functions as the main pump of the right ventricle, ejecting >85% of the stroke volume.[17] The basal portion of the right ventricle is characterized by a smooth myocardial wall, whereas the apical portion of the right ventricle is thinner and more trabeculated. Dambrauskaite et al[18] have demonstrated using 1-dimensional RV strain and strain rate that the basal segment of the RV free wall had higher deformation than the apical segments in adult patients with PH. With a significant increase in wall stress from high afterload, the apical segment becomes a passive structure and fails more profoundly than the basal segment.[18] This explains why TAPSE, a measure of longitudinal fibers and the basal segment of the right ventricle, may still be normal in patients with PH when the apical portions of their right ventricles are not working. Hauck et al demonstrated that pediatric patients with APAH-CHD have lower TAPSE than pediatric patients with IPAH because of cardiopulmonary bypass rather than PH.[19] We found similar TAPSE results in our patients with APAH-CHD when compared with the results in patients with IPAH. We also found that the global circumferential strain is decreased in patients with IPAH when compared with that in patients with APAH-CHD. Specifically, the circumferential strain at the apex free wall is decreased in patients with PH compared with that in controls and also worse in patients with IPAH than in patients with APAH-CHD. Patients with IPAH tend to have worse disease than patients with APAH-CHD; thus, when the right ventricle starts to fail, its apex is the earliest portion to be affected. Furthermore, Driessen et al[20] demonstrated that in children with IPAH, there is apical remodeling with highly inefficient RV kinetics. In patients with IPAH, the

Preprint version accepted to appear in The *Journal of Heart and Lung Transplantation*.
Final version of this paper available at https://www.sciencedirect.com/science/article/abs/pii/S1053249820318313

right ventricle is more dilated than in patients with pulmonary stenosis and remodels to a spherical shape.[20] Driessen et al[20] reported that this dilation in patients with IPAH is more pronounced at the apical segment than the apical segment of patients with pulmonary stenosis. Similarly, Dambrauskaite et al[18] study showed that this decreased apical RV function is related to disease severity in PH. Decreased deformation at the apical region provides insight into the mechanism of RV failure when the right ventricle is faced with a high afterload.

The 3D RV regional deformation can provide prognostic information on patients with PAH as observed in our study mainly in the apical region. Addetia et al[8] demonstrated using curvature computations that the apical free wall is more flattened in adult patients with PH than in controls. Leary et al[21] have described that in a pressure-overloaded state, the apical bulging and the overall rounding of the RV apex occur when comparing patients with PH with controls. The loss of the circumferential strain at the apex free wall in our study was associated with worse survival. This is consistent with previous studies that the apex of the right ventricle is the first to decline in systolic function when patients are faced with a pressure-overloaded state.[14,18,20,22] The global RVLS did not emerge as an outcome predictor in this study with the exception of the longitudinal strain at the RV apex free wall, indicating that the apex is the most affected when there is RV dysfunction. When comparing circumferential strain at the apex free wall with RV EF, the AUC was higher for circumferential strain apex free wall at 24 months, although c-statistics did not demonstrate that circumferential strain appeared superior to RV EF. Our study showed that global apex free-wall area strain was predictive of outcomes in univariate analysis, consistent with previous adult PH studies.[9,10] However, in a multivariate analysis, the circumferential strain at the apex free wall was predictive of outcomes. Together, these findings indicate that strain at the apex free wall is the driver of RV dysfunction. This regional analysis

Preprint version accepted to appear in The *Journal of Heart and Lung Transplantation*.
Final version of this paper available at https://www.sciencedirect.com/science/article/abs/pii/S1053249820318313

points toward earlier detection of abnormal RV deformation at the apex and provides an understanding of the mechanism of RV dysfunction when faced with high afterload in pediatric patients with PAH.

Limitations:

Image quality was limited by the large size probe of the Siemens machine used in pediatric patients. Despite this limitation, single-beat 3DE acquisition generated from the Siemens machine has a higher volume rate than those of other vendor machines and does not require breath holds in children to prevent stitch artifacts in volume acquisitions. The development of a pediatric 3D transthoracic probe for single-beat acquisition could help resolve the technical limitations. Another limitation is that 3D RV area strain computations are still done with custom software on a research station; however, with increasing advances in technology, 3D RV area strain may be brought into clinical practice because it can provide important prognostic information to understand the mechanisms of RV failure. The large variance and overlap among the groups in regional strain may limit the clinical applicability of these measurements. Nonetheless, they shed light on the mechanistic differences in this population because previous adult studies have shown the reproducibility of these strain measures.[9,23] There were only 2 outcomes in the APAH-CHD group, so the association observed in the outcome analysis may or may not apply to the APAH-CHD group. However, in pediatric PH studies, IPAH and APAH-CHD are frequently combined in the study to increase the number of patients in this rare disease. Combining these 2 groups is representative of the population of children in PH referral centers and previous research papers.[2,24–26]

Preprint version accepted to appear in The *Journal of Heart and Lung Transplantation*.
Final version of this paper available at https://www.sciencedirect.com/science/article/abs/pii/S1053249820318313

CONCLUSIONS

RV regional and global strain differ between controls and patients with PAH. RV apical free-wall area strain provides insight into the mechanism of RV dysfunction in pediatric patients with PAH, with regional strain emerging as outcome predictors, suggesting that this novel measure may be considered as a future measure of RV function.

Disclosure statement:

The authors thank Berthold Klas for his guidance in using the 3-dimensional software.

This study is supported by the Jayden DeLuca Foundation, the Leah Bult Foundation, and the Frederick and Margaret L Weyerhaeuser Foundation. This study is also supported by the National Institutes of Health/National Center for Advancing Translational Sciences Colorado Clinical and Translational Science Awards Grant Number UL1 TR002535.

Preprint version accepted to appear in The *Journal of Heart and Lung Transplantation*.
Final version of this paper available at https://www.sciencedirect.com/science/article/abs/pii/S1053249820318313

References

1. Abman SH, Hansmann G, Archer SL, et al.: Pediatric Pulmonary Hypertension: Guidelines From the American Heart Association and American Thoracic Society. Circulation 2015;132:2037-99.

2. Jone PN, Schafer M, Pan Z, Bremen C, Ivy DD: 3D echocardiographic evaluation of right ventricular function and strain: a prognostic study in paediatric pulmonary hypertension. Eur Heart J Cardiovasc Imaging 2018;19:1026-33.

3. Okumura K, Humpl T, Dragulescu A, Mertens L, Friedberg MK: Longitudinal assessment of right ventricular myocardial strain in relation to transplant-free survival in children with idiopathic pulmonary hypertension. J Am Soc Echocardiogr 2014;27:1344-51.

4. Fine NM, Chen L, Bastiansen PM, et al.: Outcome prediction by quantitative right ventricular function assessment in 575 subjects evaluated for pulmonary hypertension. Circ Cardiovasc Imaging 2013;6:711-21.

5. Rajagopal S, Forsha DE, Risum N, et al.: Comprehensive assessment of right ventricular function in patients with pulmonary hypertension with global longitudinal peak systolic strain derived from multiple right ventricular views. J Am Soc Echocardiogr 2014;27:657-65 e3.

6. Forsha D, Risum N, Kropf PA, et al.: Right ventricular mechanics using a novel comprehensive three-view echocardiographic strain analysis in a normal population. J Am Soc Echocardiogr 2014;27:413-22.

7. Addetia K, Maffessanti F, Muraru D, et al.: Morphologic Analysis of the Normal Right Ventricle Using Three-Dimensional Echocardiography-Derived Curvature Indices. J Am Soc Echocardiogr 2018;31:614-23.

Preprint version accepted to appear in The *Journal of Heart and Lung Transplantation*.
Final version of this paper available at https://www.sciencedirect.com/science/article/abs/pii/S1053249820318313

8. Addetia K, Maffessanti F, Yamat M, et al.: Three-dimensional echocardiography-based analysis of right ventricular shape in pulmonary arterial hypertension. Eur Heart J Cardiovasc Imaging 2016;17:564-75.

9. Moceri P, Duchateau N, Baudouy D, et al.: Three-dimensional right-ventricular regional deformation and survival in pulmonary hypertension. Eur Heart J Cardiovasc Imaging 2018;19:450-8.

10. Smith BC, Dobson G, Dawson D, Charalampopoulos A, Grapsa J, Nihoyannopoulos P: Three-dimensional speckle tracking of the right ventricle: toward optimal quantification of right ventricular dysfunction in pulmonary hypertension. J Am Coll Cardiol 2014;64:41-51.

11. Galie N, Barbera JA, Frost AE, et al.: Initial Use of Ambrisentan plus Tadalafil in Pulmonary Arterial Hypertension. The New England journal of medicine 2015;373:834-44.

12. Uno H, Cai T, Pencina MJ, D'Agostino RB, Wei LJ: On the C-statistics for evaluating overall adequacy of risk prediction procedures with censored survival data. Stat Med 2011;30:1105-17.

13. Vitarelli A, Mangieri E, Terzano C, et al.: Three-dimensional echocardiography and 2D-3D speckle-tracking imaging in chronic pulmonary hypertension: diagnostic accuracy in detecting hemodynamic signs of right ventricular (RV) failure. J Am Heart Assoc 2015;4:e001584.

14. Ryo K, Goda A, Onishi T, et al.: Characterization of right ventricular remodeling in pulmonary hypertension associated with patient outcomes by 3-dimensional wall motion tracking echocardiography. Circ Cardiovasc Imaging 2015;8.

Preprint version accepted to appear in The *Journal of Heart and Lung Transplantation*.
Final version of this paper available at https://www.sciencedirect.com/science/article/abs/pii/S1053249820318313

15. Satriano A, Pournazari P, Hirani N, et al.: Characterization of Right Ventricular Deformation in Pulmonary Arterial Hypertension Using Three-Dimensional Principal Strain Analysis. J Am Soc Echocardiogr 2019;32:385-93.

16. Ho SY, Nihoyannopoulos P: Anatomy, echocardiography, and normal right ventricular dimensions. Heart 2006;92 Suppl 1:i2-13.

17. Geva T, Powell AJ, Crawford EC, Chung T, Colan SD: Evaluation of regional differences in right ventricular systolic function by acoustic quantification echocardiography and cine magnetic resonance imaging. Circulation 1998;98:339-45.

18. Dambrauskaite V, Delcroix M, Claus P, et al.: Regional right ventricular dysfunction in chronic pulmonary hypertension. J Am Soc Echocardiogr 2007;20:1172-80.

19. Hauck A, Guo R, Ivy DD, Younoszai A: Tricuspid annular plane systolic excursion is preserved in young patients with pulmonary hypertension except when associated with repaired congenital heart disease. Eur Heart J Cardiovasc Imaging 2017;18:459-66.

20. Driessen MMP, Meijboom FJ, Hui W, Dragulescu A, Mertens L, Friedberg MK: Regional right ventricular remodeling and function in children with idiopathic pulmonary arterial hypertension vs those with pulmonary valve stenosis: Insights into mechanics of right ventricular dysfunction. Echocardiography 2017;34:888-97.

21. Leary PJ, Kurtz CE, Hough CL, Waiss MP, Ralph DD, Sheehan FH: Three-dimensional analysis of right ventricular shape and function in pulmonary hypertension. Pulm Circ 2012;2:34-40.

22. Moceri P, Bouvier P, Baudouy D, et al.: Cardiac remodelling amongst adults with various aetiologies of pulmonary arterial hypertension including Eisenmenger syndrome-implications on

Preprint version accepted to appear in The *Journal of Heart and Lung Transplantation*.
Final version of this paper available at https://www.sciencedirect.com/science/article/abs/pii/S1053249820318313

survival and the role of right ventricular transverse strain. Eur Heart J Cardiovasc Imaging 2017;18:1262-70.

23. Moceri P, Duchateau N, Gillon S, et al.: Three-dimensional right ventricular shape and strain in congenital heart disease patients with right ventricular chronic volume loading. Eur Heart J Cardiovasc Imaging 2020.

24. Barst RJ, McGoon MD, Elliott CG, Foreman AJ, Miller DP, Ivy DD: Survival in childhood pulmonary arterial hypertension: insights from the registry to evaluate early and long-term pulmonary arterial hypertension disease management. Circulation 2012;125:113-22.

25. Jone PN, Schafer M, Li L, Craft M, Ivy DD, Kutty S: Right Atrial Deformation in Predicting Outcomes in Pediatric Pulmonary Hypertension. Circ Cardiovasc Imaging 2017;10.

26. Haworth SG, Hislop AA: Treatment and survival in children with pulmonary arterial hypertension: the UK Pulmonary Hypertension Service for Children 2001-2006. Heart 2009;95:312-7.

Preprint version accepted to appear in The *Journal of Heart and Lung Transplantation*.
Final version of this paper available at https://www.sciencedirect.com/science/article/abs/pii/S1053249820318313

Table 1: Patients baseline characteristics

	APAH-CHD (N=47)	IPAH (N=45)	Controls (N=48)	p-value
Age (yrs.)	7.5 ± 4.7	10.7 ± 4.9	9.6 ± 5.0	p = 0.002
Female (%)	18 (38%)	30 (67%)	22 (46%)	p = 0.006
BSA (m^2)	0.9 ± 0.4	1.2 ± 0.4	1.2 ± 0.5	p = 0.002
WHO-FC				
I	29 (64.4%)	13 (28.8%)		p = 0.01
II	11 (24.4%)	22 (48.8%)		p = 0.01
III	5 (11.6%)	7 (15.5%)		p = 0.01
IV	0 (0.0%)	3 (6.7%)		p = 0.01
Medications				
PDE5i	23 (48.9%)	36 (80.0%)		p = 0.001
IV Treprostinil	0 (0.0%)	9 (20.0%)		p = 0.001
SC Treprostinil	2 (4.3%)	1 (2.2%)		p = 0.58
Inhaled Treprostinil	2 (4.3%)	3 (4.1%)		p = 0.61
IV Epoprostenol	0 (0.0%)	1 (2.2%)		p = 0.30
ERA	9 (19.1%)	27 (60.0%)		p < 0.001
CCB	4 (8.5%)	7 (15.6%)		p = 0.29
Echo Parameters				
Heart Rate (bpm)	88.7 ± 23.2	85.0 ± 20.2	78.1 ± 21.3	p = 0.082
TAPSE (cm)	1.5 ± 0.5	2.0 ± 0.5	1.9 ± 0.4	p < 0.001
RVSP estimate from TR velocity (mmHg)	38.4 ± 19.4	71.5 ± 29.6	16.6 ± 3.6	p < 0.001
3D RV EF (%)	47.5 ± 5.4	43.9 ± 7.4	55.4 ± 4.4	p < 0.001
Hemodynamics				
SPAP (mmHg)	50.2 ± 22.8	61.0 ± 22.7		p = 0.03
MPAP (mmHg)	30.8 ± 17.4	40.9 ± 17.4		p = 0.03
PVRi (WU)	6.1 ± 6.1	10.0 ± 6.2		p = 0.02

Abbreviations: 3D, 3-dimensional; APAH, associated pulmonary arterial hypertension; bpm, beats per minute; BSA, body surface area; CCB, calcium channel blockers; CHD, congenital heart disease; ECHO, echocardiogram; EF, ejection fraction; ERA, endothelin receptor antagonist; IPAH, idiopathic pulmonary arterial hypertension; IV, intravenous; MPAP, mean pulmonary artery pressure; PDEi, phosphodiesterase enzyme inhibitors; PVRi, pulmonary vascular resistance index; RV, right ventricle; RVSP, right ventricular systolic pressure; SC, subcutaneous; SPAP, systolic pulmonary artery pressure; TAPSE, tricuspid annular plane systolic excursion; TR, tricuspid regurgitation; WHO FC, World Health Organization Functional

Classifications; WU, wood unit.

Data are represented as mean ± SD; p-values are from Student's t-test for continuous variables and chi-square test for categorical variable for comparing patients with APAH-CHD with those with IPAH.

Preprint version accepted to appear in The *Journal of Heart and Lung Transplantation*.
Final version of this paper available at https://www.sciencedirect.com/science/article/abs/pii/S1053249820318313

Table 2: Parametric analysis of variance of right ventricular regional and global strain.

RV regional and global strain parameters	APAH-CHD, Mean ± SD	IPAH, Mean ± SD	Controls, Mean ± SD	p-value, Omnibus F test	p-value, APAH-CHD vs. Controls	p-value, IPAH vs. Controls	p-value, APAH-CHD vs. IPAH
Area Strain (%)							
RVOT septum	-19.1 ± 7.3	-17.6 ± 10.9	-18.4 ± 7.4	0.701	0.682	0.658	0.400
RVIT septum	-18.7 ± 7.0	-14.9 ± 9.7	-19.8 ± 9.3	**0.023**	0.550	**0.009**	**0.041**
Body septum	-26.7 ± 7.6	-26.1 ± 10.5	-32.8 ± 8.7	**<.001**	**0.001**	**<.001**	0.729
Apex septum	-20.6 ± 8.4	-20.6 ± 11.2	-32.4 ± 9.3	**<.001**	**<.001**	**<.001**	0.996
Apex free wall	-24.5 ± 5.6	-21.4 ± 9.2	-27.8 ± 6.2	**<.001**	**0.025**	**<.001**	**0.037**
Body free wall	-31.8 ± 7.2	-28.8 ± 12.3	-43.0 ± 7.8	**<.001**	**<.001**	**<.001**	0.123
RVIT free wall	-26.8 ± 7.8	-23.3 ± 10.1	-27.5 ± 8.8	0.053	0.715	**0.024**	0.057
RVOT free wall	-14.7 ± 4.7	-13.8 ± 5.8	-17.1 ± 7.1	**0.024**	**0.048**	**0.009**	0.494
Global	-24.8 ± 4.8	-22.3 ± 8.5	-29.8 ± 6.0	**<.001**	**<.001**	**<.001**	0.075
Circumferential Strain (%)							
RVOT septum	-14.6 ± 7.3	-12.5 ± 9.7	-8.6 ± 6.7	**0.002**	**<.001**	**0.022**	0.206
RVIT septum	-12.9 ± 4.9	-9.5 ± 7.5	-13.9 ± 7.8	**0.007**	0.487	**0.003**	**0.019**
Body septum	-13.1 ± 5.2	-11.3 ± 5.3	-17.2 ± 6.0	**<.001**	**<.001**	**<.001**	0.114
Apex septum	-10.3 ± 4.3	-9.9 ± 4.5	-13.7 ± 5.8	**<.001**	**<.001**	**<.001**	0.701
Apex free wall	-13.1 ± 3.9	-10.3 ± 5.3	-12.7 ± 4.4	**0.007**	0.736	**0.010**	**0.004**
Body free wall	-18.5 ± 4.8	-16.6 ± 7.2	-21.4 ± 4.7	**<.001**	**0.014**	**<.001**	0.104
RVIT free wall	-15.5 ± 5.0	-12.3 ± 5.9	-16.1 ± 4.9	**0.001**	0.560	**<.001**	**0.004**
RVOT free wall	-9.1 ± 3.9	-7.9 ± 4.4	-8.7 ± 5.0	0.453	0.666	0.412	0.216
Global	-14.3 ± 3.4	-12.1 ± 5.0	-15.5 ± 3.9	**<.001**	0.179	**<.001**	**0.010**
Longitudinal Strain (%)							
RVOT septum	-4.2 ± 5.4	-3.8 ± 5.0	-9.9 ± 5.4	**<.001**	**<.001**	**<.001**	0.676

Preprint version accepted to appear in The *Journal of Heart and Lung Transplantation*.
Final version of this paper available at https://www.sciencedirect.com/science/article/abs/pii/S1053249820318313

RV regional and global strain parameters	APAH-CHD, Mean ± SD	IPAH, Mean ± SD	Controls, Mean ± SD	p-value, Omnibus F test	p-value, APAH-CHD vs. Controls	p-value, IPAH vs. Controls	p-value, APAH-CHD vs. IPAH
RVIT septum	-6.6 ± 6.2	-5.2 ± 6.9	-6.2 ± 7.2	0.603	0.806	0.465	0.333
Body septum	-15.0 ± 6.4	-15.4 ± 7.7	-18.3 ± 6.2	**0.038**	**0.019**	**0.043**	0.758
Apex septum	-11.8 ± 7.2	-12.0 ± 9.1	-22.1 ± 7.8	**<.001**	**<.001**	**<.001**	0.908
Apex free wall	-13.4 ± 4.2	-12.3 ± 5.8	-17.1 ± 4.3	**<.001**	**<.001**	**<.001**	0.283
Body free wall	-15.5 ± 6.9	-14.4 ± 7.6	-26.7 ± 6.6	**<.001**	**<.001**	**<.001**	0.459
RVIT free wall	-12.7 ± 6.9	-11.5 ± 6.5	-12.0 ± 8.1	0.715	0.622	0.743	0.418
RVOT free wall	-6.5 ± 3.2	-6.0 ± 2.9	-8.7 ± 4.3	**<.001**	**0.004**	**<.001**	0.443
Global	-11.9 ± 3.5	-11.1 ± 4.6	-16.4 ± 3.8	**<.001**	**<.001**	**<.001**	0.330

Abbreviations: ANOVA, analysis of variance; APAH, associated pulmonary arterial hypertension; CHD, congenital heart disease; IPAH, idiopathic pulmonary arterial hypertension; RV, right ventricular; RVIT, right ventricular inflow tract; RVOT, right ventricular outflow tract. Statistical significance is p-value <0.05 between the groups.

Preprint version accepted to appear in The *Journal of Heart and Lung Transplantation*.
Final version of this paper available at https://www.sciencedirect.com/science/article/abs/pii/S1053249820318313

Table 3: Univariate survival analysis after adjusting for age and BSA.

RV regional and global strain parameters predictors	Adjusted Hazard Ratio	Lower 95% Wald Confidence Limit	Upper 95% Wald Confidence Limit	Pr > ChiSq
Area Strain (%)				
Apex free wall	1.049	1.007	1.093	0.0228
Circumferential Strain (%)				
Apex free wall	1.098	1.021	1.181	0.0118
RVIT free wall	1.076	1.005	1.151	0.0344
Longitudinal Strain (%)				
Apex free wall	1.079	1.004	1.159	0.0388
WHO 1 vs 2	0.16	0.04	0.61	<0.001
WHO 1 vs 3	0.08	0.02	0.34	<0.001
WHO 1 vs 4	0.02	0.00	0.14	<0.001
WHO 2 vs 3	0.48	0.17	1.37	<0.001
WHO 2 vs 4	0.13	0.03	0.64	<0.001
WHO 3 vs 4	0.27	0.05	1.45	<0.001

Abbreviations: BSA, body surface area; ChiSq, chi-square; Pr, probability; RVIT, right ventricular inflow tract; RV, right ventricular; WHO, World Health Organization.

Preprint version accepted to appear in The *Journal of Heart and Lung Transplantation*.
Final version of this paper available at https://www.sciencedirect.com/science/article/abs/pii/S1053249820318313

Table 4: Cox regression analysis and Uno's concordance statistic of right ventricular regional strain parameters adjusted for age and body surface area

RV regional strain parameters	Uno's concordance statistic (SEM)	Integrated AUC of ROC curves	Adjusted Hazard Ratio (95% CI)*	Pr > ChiSq†
Circumferential strain apex free wall (%)	0.72 (0.08)	0.72	1.098 (1.021,1.181)	0.0118
Area Strain apex free wall (%)	0.73 (0.10)	0.70	1.049 (1.007, 1.093)	0.0228
Circumferential strain RVIT free wall (%)	0.67 (0.07)	0.70	1.076 (1.005, 1.151)	0.0344
Longitudinal strain Apex free wall (%)	0.70 (0.08)	0.67	1.079 (1.004, 1.159)	0.0388

Abbreviations: AUC, area under the curve; c-statistic, concordance statistic; ChiSq, chi-square; Pr, probability; ROC, receiver operating characteristic; RV, right ventricular; RVIT, right ventricular inflow tract; SEM, standard error of mean. Hazard ratio per 1 U change in the predictor.

Preprint version accepted to appear in The *Journal of Heart and Lung Transplantation*.
Final version of this paper available at https://www.sciencedirect.com/science/article/abs/pii/S1053249820318313

FIGURE LEGENDS

Figure 1: Segmentation of the RV septal and free walls into inlet, outlet, body, and apex regions. RV, right ventricular.

Figure 2: 3D area strain, circumferential strain, and longitudinal strain patterns (median pattern for each group) and statistical differences (p-value from Hotelling's T-test) among controls, patients with APAH-CHD, and patients with IPAH. 3D, 3-dimensional; APAH, associated pulmonary arterial hypertension; CHD, congenital heart disease; IPAH, idiopathic pulmonary arterial hypertension; PAH, pulmonary arterial hypertension.

Figure 3: The area strain of the apex free wall (shaded in black), the circumferential strain of the apex free wall (blue), the longitudinal strain of the apex free wall (green), and the circumferential strain of the inlet free wall (red) were predictors of adverse clinical events. RV, right ventricular.

Figure 4: ROC curves showed that the AUC for circ strain at the apex free wall was higher than those at other regions of the right ventricle at 24 months. AUC, area under the curve; BSA, body surface area; circ, circumferential; ROC, receiver operating characteristic; RV, right ventricular.

Figure 5: ROC curves showed that the AUC for Circ strain at the apex free wall was higher than that for RV EF at 24 months. AUC, area under the curve; Circ, circumferential; EF, ejection fraction; ROC, receiver operating characteristic; RV, right ventricular.

Figure 6: Time-dependent AUC when age, BSA, WHO FC, and Circ strain at the apex free wall are used in the multiple Cox regression analysis. The highest iAUC was 0.8553 with age, BSA, WHO FC, and Circ strain at the apex free wall. AUC, area under the curve; BSA, body surface area; Circ, circumferential; ECHO, echocardiogram; iAUC, integrated area under the curve; WHO, World Health Organization; WHO FC, World Health Organization Functional Classifications.

Preprint version accepted to appear in The *Journal of Heart and Lung Transplantation*.
Final version of this paper available at https://www.sciencedirect.com/science/article/abs/pii/S1053249820318313

Figure 1

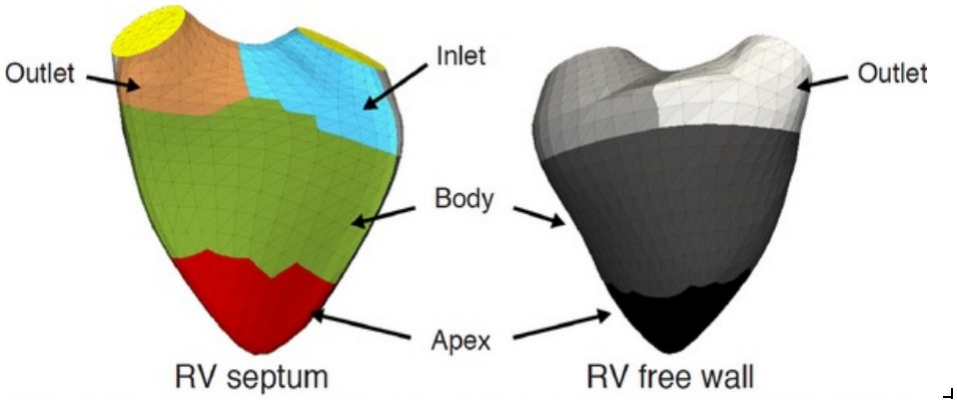

Preprint version accepted to appear in The *Journal of Heart and Lung Transplantation*.
Final version of this paper available at https://www.sciencedirect.com/science/article/abs/pii/S1053249820318313

Figure 2

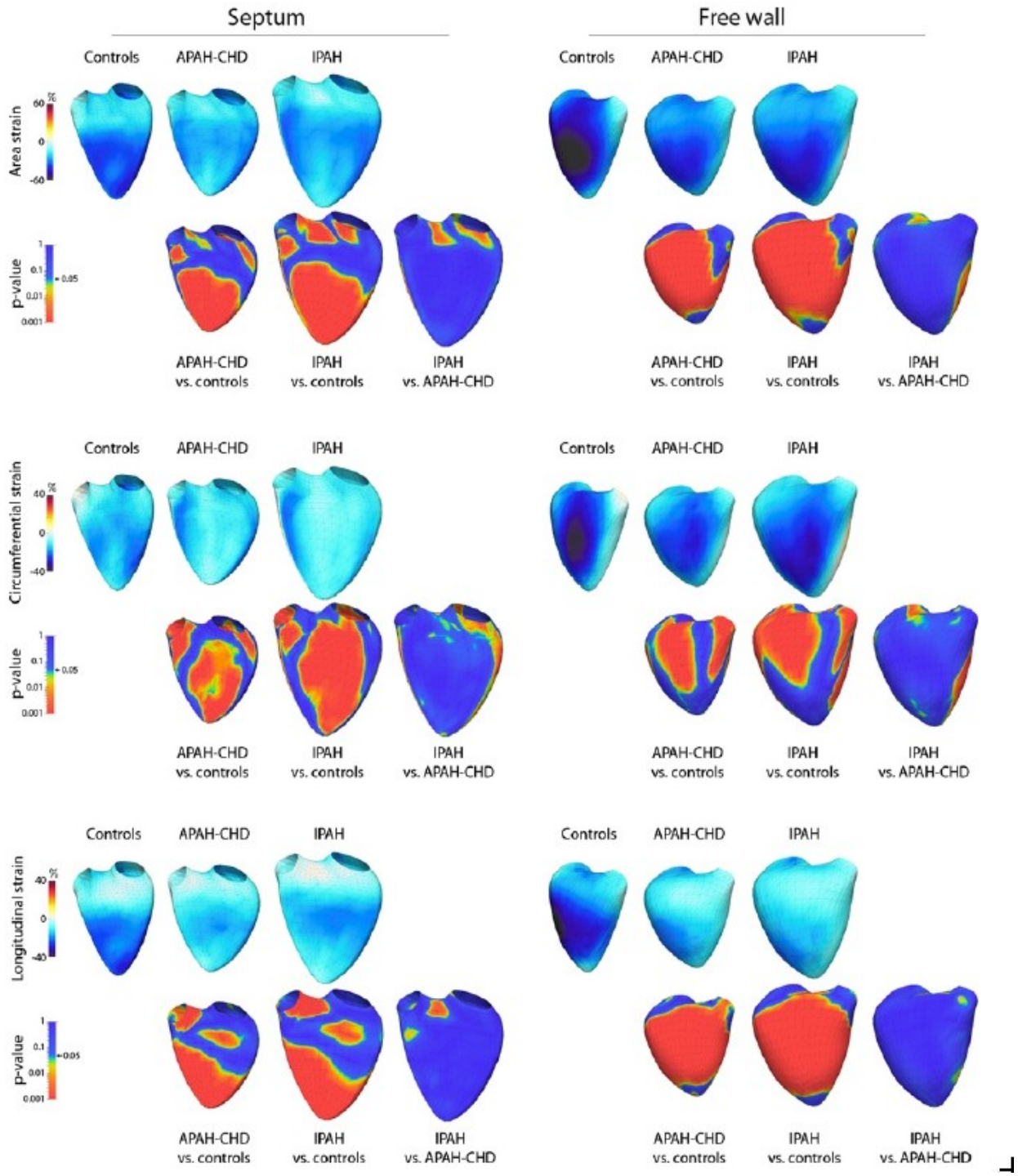

Preprint version accepted to appear in The *Journal of Heart and Lung Transplantation*.
Final version of this paper available at https://www.sciencedirect.com/science/article/abs/pii/S1053249820318313

Figure 3

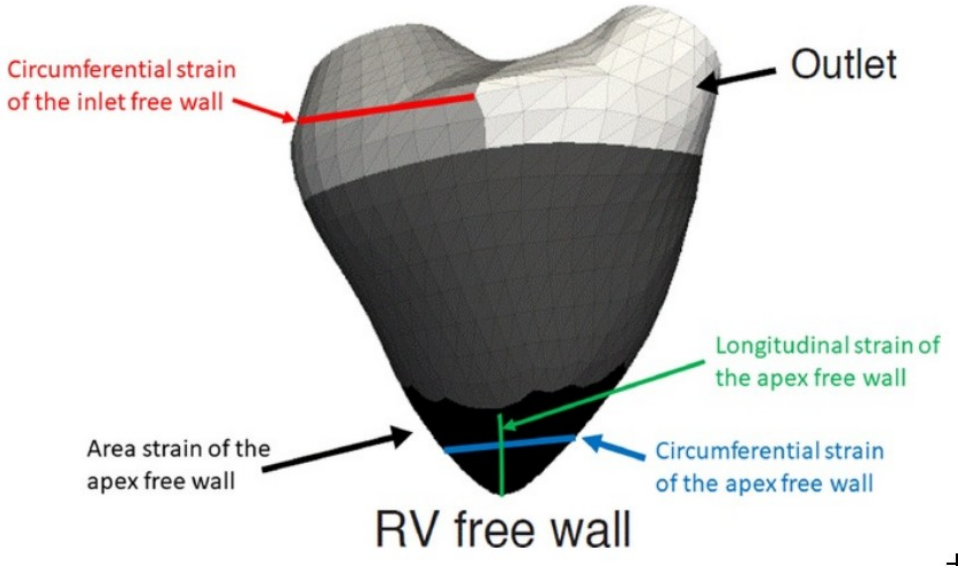

Preprint version accepted to appear in The *Journal of Heart and Lung Transplantation*.
Final version of this paper available at https://www.sciencedirect.com/science/article/abs/pii/S1053249820318313

Figure 4

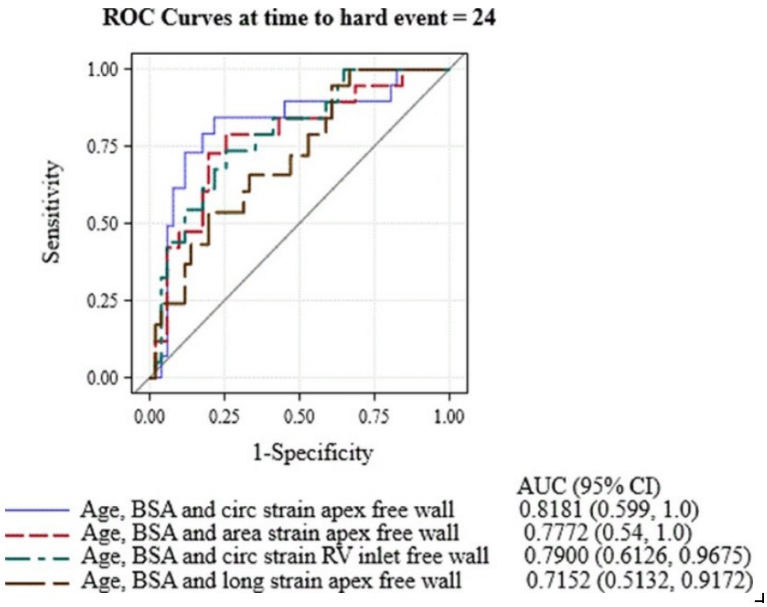

Preprint version accepted to appear in The *Journal of Heart and Lung Transplantation*.
Final version of this paper available at https://www.sciencedirect.com/science/article/abs/pii/S1053249820318313

Figure 5

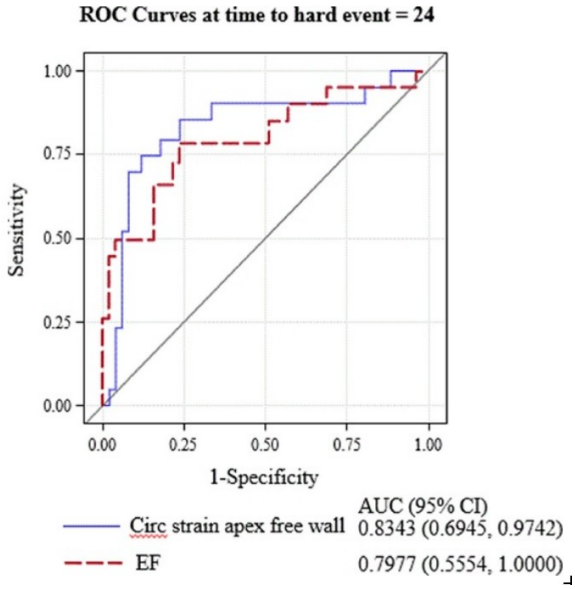

Preprint version accepted to appear in The *Journal of Heart and Lung Transplantation*.
Final version of this paper available at https://www.sciencedirect.com/science/article/abs/pii/S1053249820318313

Figure 6